

1 **Directional and frequency characteristics of auditory neurons in** 2 **Culex male mosquitoes**

3 **Dmitry. N. Lapshin¹ and Dmitry. D. Vorontsov²**

5 ¹ Institute for Information Transmission Problems of the Russian Academy of Sciences
6 (Kharkevich Institute)

7 Bolshoy Karetny per. 19, Moscow, 127994, Russia

8 E-mail: lapshin@iitp.ru

9 ² Koltzov Institute of Developmental Biology Russian Academy of Sciences

10 Vavilova 26, Moscow, 119334, Russia

11 E-mail: d.vorontsov@idbras.ru (corresponding author)

12

13 **Summary statement**

14 Auditory neurons of mosquito are grouped into pairs or triplets, each unit tuned to a
15 specific frequency. Within the pair units respond to opposite directions of the sound. Units of
16 different tuning and sensitivity are evenly distributed around the axis of the Johnston's organ.

17

18 **Abstract**

19 The paired auditory organ of mosquito, the Johnston's organ (JO), being the receiver of
20 particle velocity component of sound, is directional by its structure. However, to date almost no
21 direct physiological measurements of its directionality was done. In addition, the recent finding on
22 the grouping of the JO auditory neurons into the antiphase pairs demanded confirmation by
23 different methods. Using the vector superposition of the signals produced by two orthogonally
24 oriented speakers, we measured the directional characteristics of individual units as well as their
25 relations in physiologically distinguishable groups – pairs or triplets. The feedback stimulation
26 method allowed to discriminate responses of the two simultaneously recorded units, and to show
27 that they indeed responded in antiphase. We also show that ratios between the individual tuning
28 frequencies in pairs and triplets are non-random and follow the principle of harmonic
29 synchronization, remarkably similar to the one known from the observations of mosquito behavior.

30 Units of different tuning and sensitivity are evenly distributed around the axis of the JO, providing
31 the mosquito with the ability to produce complex auditory behaviors.

32

33 **Key words**

34 Mosquito, auditory sense, Johnston's organ, directional sensitivity, frequency tuning,
35 harmonic synchronization

36

37 **1. Introduction**

38 The ear of mosquito, the Johnston's organ (JO), is a highly sophisticated system containing
39 extremely large number of sensory neurons, measured in thousands (Boo and Richards, 1975a; Boo
40 and Richards, 1975b; Hart et al., 2011). Its complexity should not be surprising since mosquito
41 mating behavior depends on audition and hence the ears were developed under high selection
42 pressure. Morphologically, mosquito possesses two feather-like antennae, designed to be the
43 receivers of air particle velocity. The antenna originates from the capsule with the radially arranged
44 sensillae, or scolopidia, most of which contain two or three bipolar sensory neurons. The neurons
45 respond to antenna vibrations by transducing them into electrical potentials and send the axons to
46 the brain via the antennal nerve.

47 The task of reception of a mate's flight tone which lies within the narrow frequency range
48 does not seem to be too complicated at the first sight. However, the real-life task which is solved by
49 the mosquito auditory system is much more difficult. First of all, any external sound blends with
50 mosquito's own flight tone, that leads to the appearance of multiple mixed harmonics at the receptor
51 input (Gibson et al., 2010; Lapshin, 2011; Lapshin, 2012; Simões et al., 2016; Simões et al., 2018;
52 Warren et al., 2009). The flight tone itself is not stable since it depends on the ambient temperature
53 (Sotavalta, 1952; Villarreal et al., 2017), and, in addition to this, mosquitoes continuously
54 maneuver, change their flight velocity and, hence, the wingbeat frequency. This change is especially
55 remarkable during the courtship 'acoustic dance', when male mosquitoes first produce the rapid
56 frequency modulation, and then the pair of mosquitoes mutually tune their wingbeats to fit the
57 specific frequency ratio (Aldersley and Cator, 2019; Cator et al., 2009; Gibson and Russell, 2006;
58 Pennetier et al., 2010; Warren et al., 2009). A male mosquito not only needs to detect the presence
59 of a female, but has to locate her and follow until copulation. And, since many mosquitoes mate in a
60 swarm, to win the competition our male must perform these tasks faster than other males.

61 Given all this, the complexity of the mosquito JO is no more surprising. The principles of
62 its operation are still waiting to be understood, and there is no reason to consider them being trivial.
63 From the obvious tasks mentioned above one can presume that the JO must contain units tuned to
64 different frequencies and, most probably, with different sensitivity to provide high dynamic range.
65 The radially symmetrical flagellar JO is said to be inherently directional (Belton, 1974; Robert,
66 2005). At the level of sensory neurons this means that there must be sensory units selectively
67 responding to a sound coming from any angular range, but whether the sensitivity and frequency
68 preference of the JO is also symmetrical has never been tested, except several experiments made by
69 Belton (1974).

70 In the much simpler organized JO of *Drosophila* (>400 mechanosensory neurons), different
71 types of primary sensory neurons were discovered (Albert and Göpfert, 2015; Kamikouchi et al.,
72 2009; Yorozu et al., 2009), as well as interneurons which selectively code the complex stimulus
73 features (Chang et al., 2016; Matsuo and Kamikouchi, 2013). Although the *Drosophila* model
74 allows to analyze the mechanisms which are not currently accessible in mosquitoes, the results of
75 these studies should be transferred to the mosquito audition with some caution due to much higher
76 complexity of the latter and substantially different acoustic behavior in fruit flies and mosquitoes.
77 The physiological approach directed to testing the properties of the auditory neurons in mosquito
78 involves the recording of their responses to sound. However, the method of recording the field
79 potential of the whole JO, which is most commonly applied in the studies of the mosquito audition,
80 does not allow to test any hypotheses on the diverse tuning of elements within the JO, neither
81 frequency nor directional. Recently we developed a method of recording from small groups of
82 axons of the JO sensory neurons along with controlled acoustic stimulation (Lapshin and Vorontsov,
83 2013). Although even the fine glass electrode used in that study allowed recording of focal
84 potentials, still due to the extremely tiny diameter of the axons in the antennal nerve the resolution
85 of recording had to be further improved, which was done by applying the positive feedback
86 stimulation. Using it, it was possible to see the frequency preference of a unit situated closer to the
87 electrode tip or possessing the lower threshold than other units.
88 The first finding which that study brought was the difference in frequency tuning between the JO
89 sensory neurons both in female (Lapshin and Vorontsov, 2013) and male mosquitoes (Lapshin and
90 Vorontsov, 2017). It was rather expected, keeping in mind the high number of units and also the
91 behavioral observations which implied the frequency discrimination in mosquitoes (Aldersley and
92 Cator, 2019; Aldersley et al., 2016; Lapshin and Vorontsov, 2018; Simões et al., 2016; Simões et al.,
93 2018). The individual tuning frequencies were distributed from 85 to 470 Hz in males and from 40
94 to 240 Hz in females of *Culex pipiens*, while the majority of units was found to be tuned to the
95 tones other than the wingbeat frequency of a mate.

96 A rather unexpected finding, however, was that the units going closely in the antennal
97 nerve were found to be grouped in distinct pairs or triplets by the specifics of their response. In each
98 group, the ratio between the individual tuning frequencies was non-random, while the frequencies
99 themselves were distributed more or less randomly within the range of sensitivity. Moreover, the
100 units within a pair demonstrated the antiphase response to the same stimulus. Each of the proposed
101 explanations of the latter finding was nontrivial: either the axons from the opposite sectors of the JO
102 were pairwise combined in a nerve, or the two units belonged to the same sensilla, but nonetheless
103 responded in antiphase due to some specific tuning at the stage of mechanotransduction. The set of
104 non-random ratios between the individual tuning frequencies within each pair or triplet of units
105 remarkably coincided with the recent behavioral data on the mutual frequency tuning (Aldersley et
106 al., 2016). Here we study the current larger set of measurement data in attempt to understand the
107 principles behind the primary signal analysis which, as we presume, is performed by the JO sensory
108 neurons even before this information enters the brain.

109 The weakness of our previous study was in the specifics of the positive feedback
110 stimulation setup, which at that time provided only two variants of the stimulation phase: either 0°
111 or 180° relative to the unit response. This limitation did not allow to tell whether the units which
112 responded in a pair were strictly antiphase (180°), or possessed some other close directional ratio,
113 since no directional measurements were performed. This was the primary reason for us to undertake
114 another study and to utilize a different method of measuring the directional properties of the JO
115 neurons. Here, we measure the thresholds of auditory neurons of the JO as a function of orientation
116 of the acoustic wave vector relative to the axis of the antenna. Such data plotted in polar coordinates
117 is commonly referred to as the polar pattern or the directional characteristic.

118 In previous studies, the polar pattern was assessed either by changing the angular position
119 of the speaker relative to the test object (Daley and Camhi, 1988; Vedenina et al., 1998), or by
120 rotating the test object relative to the stationary speakers (Hill and Boyan, 1976; Morley et al.,
121 2012). There exists, however, a third way to study the directionality: to use a vector superposition of
122 acoustic waves at the point of receiver, produced by two orthogonally oriented stationary speakers
123 (Theunissen et al., 1996). In this study we implemented, with modifications, the latter method. It
124 allowed us to avoid the mechanical vibrations associated with the movements of objects within the
125 setup, that was in its turn important for stability of recording. Additionally, herein we compare the
126 directional characteristics measured from the same sensory units by the sinusoidal and the positive
127 feedback stimulation, and give the distribution of units with different frequency tuning around the
128 axis of the mosquito antenna.

129 The preliminary study of directional properties of the JO sensory units was done in
130 Chironomidae midges (Lapshin, 2015). Their auditory behavior is generally similar to that of
131 Culicidae: swarming males are attracted to the female wingbeat tone; morphologically their JO's
132 also have many similarities. These experiments have shown that positive feedback stimulation can
133 be successfully used to simultaneously measure the frequency and directional characteristics of the
134 JO sensory neurons.

135

136 **2. Methods**

137 The relative threshold characteristics of auditory sensory units of the JO were measured
138 depending on the orientation of acoustic wave vector relative to the axis of the antenna. In parallel,
139 the individual tuning frequencies of units were identified.

140

141 **2.1. Animal preparation**

142 Males of *Culex pipiens pipiens* L. (n=91) were captured from a natural population in
143 Moscow region of the Russian Federation. Experiments were conducted in laboratory conditions
144 with air temperature 18-21°C in at the Kropotovo biological station (54° 51' 2" N; 38° 20' 58" E).

145 Individual mosquitoes were glued to a small (10x5 mm) copper-covered triangular plate by
146 a flour paste with 0.15 M sodium chloride added. This type of attachment simultaneously serves
147 three functions: it ensures good electrical contact of the mosquito with the plate, which was used as
148 a reference electrode, mechanically fixes the mosquito and prevents it from drying during the
149 experiment. The head of the mosquito was glued to its body by a bead of varnish to keep its
150 orientation fixed during the experiment. The mosquito could still move its antennas, but this was
151 visually controlled. The plate with the mosquito was mounted on a holder using a pair of miniature
152 ferrite magnets which allowed to position the mosquito at any desired angle relative to the speakers.
153 In most experiments the mosquito was positioned dorsal side up. However, the constant orientation
154 of mosquito relative to the recording electrode could result in selective recording of some particular
155 groups of neurons. To avoid this kind of a bias, the orientation was changed from specimen to
156 specimen, either by turning it the ventral side up or by rotating it by 180° in the horizontal plane;
157 measurements of directional responses were corrected accordingly. All recordings were made from
158 the left JO.

159

160 **2.2. Acoustic stimulation**

161 Sound stimuli were delivered through a pair of Scandinavia 75 dynamic speakers (DLS,
162 Sweden) positioned with their acoustic axes at the right angle (Fig. 1). The mosquito was fixed at
163 the intersection of these axes in such a way that the base of the antenna flagellum and the axis of the
164 associated JO was perpendicular to the plane defined by the axes of the two speakers.

165 The speakers were powered from the home-made amplifier ($K = 4$) via a passive Sin–Cos
166 (SC) transducer which produced two derived signals with the amplitudes,

$$167 \quad A_1 = 0.25 \cdot U \cdot \cos\left(\frac{\pi}{180} \cdot (\phi + 45)\right)$$

$$168 \quad A_2 = 0.25 \cdot U \cdot \sin\left(\frac{\pi}{180} \cdot (\phi + 45)\right)$$

169 where A_1 and A_2 are the amplitudes of the control signals for the first and the second
170 speaker, respectively; U is the alternating voltage at the input of the SC transducer; ϕ is the angle
171 between the dorso-ventral line passing through the mosquito's head and the vector of vibration
172 velocity of air particles. An increase in ϕ corresponds to counter-clockwise rotation of the velocity
173 vector, with the insect's head viewed from the front (Fig. 1). Accordingly, when viewed from the
174 mosquito's head along the antenna the clockwise rotation corresponds to the increase in ϕ .

175 The resulting direction of the air vibration velocity in the stimulating system was
176 determined by the vector superposition of the signals from both speakers. Changes in the sound
177 wave direction relative to the mosquito in 15° ($\pi/8$) steps were accomplished by coordinated
178 switching of voltage dividers in the SC transducer. For those angles at which the values of the
179 functions $\sin(\phi+45)$ or $\cos(\phi+45)$ were negative, the signal polarity was inverted by switching the
180 terminals of the speakers. This technique of variation of the sound wave vectors did not require any
181 construction elements to be moved inside the test zone during the experiment, so it allowed to avoid
182 vibrations which could affect the focal microelectrode recordings and, in addition, the
183 measurements could be made faster compared to the techniques which involve the rotation of the
184 speaker or the animal.

185 The moving parts of the speaker had a low resonant frequency (90 Hz). Due to the
186 considerable response lag of the dome of the speaker and its support, the emission phase delay
187 increased with the signal frequency up to the point of inversion. To stabilize the phase delay, a
188 phase correction depending on the stimulation frequency was included in the speaker control circuit.

189 The sinusoidal stimuli were generated by the digital-to-analog converter LA-DACn10m1
190 (Rudnev-Shilyaev, Russian Federation). Acoustic calibration of the stimulating device was

191 performed with an NR-231-58-000 differential capacitor microphone (Knowles Electronics, USA)
192 attached to a micropositioner with axial rotation feature and set in the position of the mosquito. The
193 same microphone put in 2 cm from the mosquito was used to record the stimulation signals during
194 the recordings.

195 The differential microphone together with its amplifier was previously calibrated in the far
196 field using the B&K 2253 sound level meter with a B&K 4135 microphone (Brüel & Kjær,
197 Denmark). All sound level data in this study are given in the logarithmic scale in dB RMS SPVL
198 (root mean square sound particle velocity level), with a reference level of 0 dB being equal to
199 4.85×10^{-5} mm/s, which corresponds in the far field to the standard reference sound pressure of
200 20 μ Pa.

201

202 **2.3. Microelectrode recordings**

203 Focal recordings from the axons of the antennal nerve were made with glass
204 microelectrodes (1B100F-4, WPI Inc.) filled with 0.15 M sodium chloride and inserted at the
205 scape-pedicle joint. In this study we preferred the extracellular responses to the quasi-intracellular
206 ones due to the stability of the former over a long time interval required for directional
207 measurements.

208 After the penetration of the cuticle electrodes had a resistance of 15–110 M Ω . The
209 electrode was manipulated by means of micropositioner. The whole setup was mounted at the
210 vibration-isolated steel table. Neuronal responses were amplified using a home-made DC amplifier
211 (gain 10, input resistance >10 G Ω). To use the neuronal responses for feedback stimulation (see
212 below) and to measure the response thresholds, the output of the DC amplifier was passed through
213 an additional AC amplifier (gain 20, 30 or 40 dB, band-pass = 5–5000 Hz). Responses and
214 stimulation signals were digitized using E14-440 A/D board (L-Card, Russian Federation) at
215 20 kHz sampling rate, and LGraph2 software. Digitized recordings were examined with Sound
216 Forge Pro 10 (Sony).

217 Due to the fact that the electrode tip and the average diameter of sensory axon in the antennal nerve
218 were of comparable size (1 μ m or less), we cannot claim that the recordings were made from the
219 individual axons. For the sake of simplicity, here we use the terms 'unit' or 'sensory unit' in the sense
220 of one or several axons belonging to the primary sensory neurons of the JO, closely located within
221 the antennal nerve and sharing similar frequency and phasic properties, thus representing a single
222 functional unit. Detailed discussion of this issue can be found elsewhere (Lapshin and Vorontsov,
223 2013; Lapshin and Vorontsov, 2017)

224 **2.4. Measurements of the directional sensitivity**

225 While penetrating the antennal nerve by the electrode, the preparation was continuously
226 stimulated with tonal pulses (filling frequency 200–260 Hz, amplitude 60–65 dB SVPL, duration 80
227 ms, period 600 ms). During this searching procedure the groups of the JO neurons situated
228 orthogonal to the antenna oscillation could be overlooked. To avoid this, the vector of acoustic wave
229 was periodically changed by 90° using the switch on the SC transducer.

230 The threshold measurements were made using either sinusoidal (to obtain absolute
231 thresholds) or the positive feedback stimulation (to obtain relative thresholds). The essence of the
232 latter method is a positive feedback loop established using the amplified in-phase response of a
233 sensory unit as the signal to drive the stimulation loudspeaker. Applying such kind of stimulation to
234 the sensory unit we expect it to 'sing' at a frequency which is close to its intrinsic tuning frequency –
235 we call this effect 'autoexcitation'. With feedback stimulation, the threshold was defined as the
236 signal level which required one more incremental step at the attenuator output (+1 dB) for the
237 system to enter the autoexcitation mode. With sinusoidal stimulation, the criterion of the response
238 threshold was set at 2 dB of sustained excess of response amplitude above the average noise level in
239 a given recording. At each combination of stimulation parameters the threshold was measured
240 consequently at least twice.

241 To distinguish between the two above methods, hereinafter we will use the term 'polar
242 patterns' for the results obtained by the positive feedback stimulation, and 'directional
243 characteristics' for those measured with sinusoidal stimulation. It is important to bear in mind that
244 the feedback method provides the unipolar response, i. e. it allows to distinguish between the two
245 units responding to the opposite (180°) phases of the antenna vibration. The directional
246 characteristics obtained using the sinusoidal stimulation are always bipolar.

247 The directional characteristics and polar patterns of sensory neurons were obtained by
248 measuring the auditory thresholds at different angles of acoustic stimulation vector which was
249 changed in 15° steps. Since the complete set of measurements took quite a long time (20–25 min),
250 repeated measurements at certain angles (usually at 45° and 315°) were made not less than twice
251 per measurement series to ascertain the stability of recording.

252 During the subsequent data processing, the maximum threshold value (Th_{max}) was
253 determined for a given recorded unit. Based on it, a set of derived values describing the unit
254 directional characteristic or polar pattern was estimated by the formula $A_i = Th_{max} - Th_i$. In the
255 curves based on these data, the sectors of the highest sensitivity corresponded to the lowest recorded

256 thresholds, and the central zero point corresponded to Th_{max} . The angles at which no response at the
257 best frequency was observed were given the value $A_i = 0$.

258 The angular sensitivity range of a unit was determined at -6 dB of the maximum
259 sensitivity (in case of directional characteristics the two values from the symmetrical curves were
260 averaged). The best angle of a given unit was determined as the bisector of this range.

261 Since it is known that frequency tuning of the JO, as well as the wingbeat frequency,
262 highly depend on the ambient temperature (Costello, 1974; Villarreal et al., 2017), all the frequency
263 data in this study underwent temperature correction to the value of 20°C . For such calculations, the
264 previously estimated coefficient of 0.02 Hz per 1°C was used.

265

266 **3. Results**

267 **3.1. Individual directional properties of the JO units**

268 As a rule, in one specimen directional measurements were made consecutively from two or
269 more recording sites within the antennal nerve. At each recording site the polar pattern of one unit
270 (if a single unit was responding), two (in most cases) or three units was measured together with
271 their tuning frequencies in the mode of feedback stimulation. Then, in case of a stable recording, the
272 directional characteristics of the same unit(s) were measured using the sinusoidal stimulation.
273 Recordings were made from 91 male mosquitoes. In total, directional properties of 306 units were
274 measured in the frequency range $114\text{--}359$ Hz, among them there were 46 single, 85 paired (two
275 units recorded together but responding in antiphase) and 30 tripled units. In the latter group of
276 recordings, two units responded in-phase, but demonstrated different frequency tuning, and one
277 responded in antiphase and was tuned to the third frequency lying between the ones of the in-phase
278 pair.

279 The examples of individual responses are shown in Fig.2. We do not show the waveforms here, they
280 were similar to the ones described in detail elsewhere (Lapshin and Vorontsov, 2017).

281 When the power of the feedback was increased from the sub-threshold levels, first a higher
282 level of noise appeared (Fig.2A), followed by sporadic bursts of activity (from -1 to 0 dB in the
283 shown example). At higher levels of feedback the response transformed into continuous excitation
284 at the specific frequency, often with higher harmonics also present in the recording. When the
285 direction of the sound wave was switched to the opposite, the kind of response was similar, but the
286 unit(s) excited at the different frequency. We observed this effect in the previous studies when

287 switching the phase of the signal in the feedback circuit, although here the change of the sound
288 wave direction was done in a different way.

289 Alternatively, when the feedback power was kept stable above the threshold, and the vector
290 of acoustic wave was rotated stepwise, the excitation gradually appeared and disappeared
291 depending on the angle of stimulation. In triple unit recordings at certain angles two frequencies
292 were present simultaneously, producing the combination, or mixed harmonics (Fig.2B).

293 In case of paired unit recording their individual polar patterns were opposite ($180^\circ \pm 10^\circ$),
294 mirroring each other, while their individual tuning frequencies were different (Fig3. A). For the
295 same pair of units, the directional characteristic measured on the best frequency was bi-directional
296 (figure-eight pattern) with its axis with slight deviation following the axis of previously measured
297 combined polar patterns (Fig3. B). Angular orientation of polar patterns at the given recording site
298 was arbitrary, with no obvious preference across the antennal nerve. Usually, after a slight axial
299 shift of the electrode another pair or triplet of units started to respond, demonstrating different
300 angular orientation and different tuning frequencies while maintaining the opposite, mirror-like
301 polar patterns. The polar pattern of a single unit had the form of a petal located asymmetrically
302 relative to the center of polar coordinates. One of the possible reasons for appearance of single-unit
303 recordings may be the mechanical instability of the preparation due to the muscle contractions. In
304 other words, some of the experiments ceased before the measurements from all directions were
305 made. However, not all recordings with only a single unit responding can be explained in such a
306 way.

307 Sometimes the ordinary petal shape of the polar pattern was distorted in the form of one or
308 two notches appearing in it (Fig.3C). Directional characteristics measured from the same units
309 demonstrated some similarity in shape (Fig.3D). Such distortions can be explained by the presence
310 of additional antiphase units in the area of focal recording, and their effect on the recording quite
311 predictably was more pronounced during the feedback stimulation and the polar pattern
312 measurements.

313 The average angular sensitivity range of a unit, measured from directional characteristics at
314 -6 dB from the maximum, was found to be 123° ($\sigma=14.5^\circ$, $n=74$). The same, estimated from the
315 polar patterns, was slightly narrower: 100° ($\sigma=16^\circ$, $n=275$). This difference in estimates is easily
316 explained, since the positive feedback, on which the measurements of the polar patterns were based,
317 was very sensitive to the decrease in transfer coefficient, and this effect had to be most significant at
318 the directions of minimal sensitivity of the unit.

319

320 The absolute thresholds of sensitivity at best frequencies varied from 22 to 44 dB SPVL
321 (M=32 dB SPVL, $\sigma=4.4$ dB, n=74).

322 **3.2. Directional characteristics of the JO**

323 Both frequency tuning and individual sensitivity of units were found to be more or less
324 evenly distributed around the antenna (Fig. 4). Some asymmetry in the angular distribution of units
325 can be explained by the difference in the total numbers of units recorded in each sector (1 and 3 vs 2
326 and 4 in Fig. 4A). The absolute thresholds of sensitivity at best frequencies varied from 22 to 44 dB
327 SPVL (M=32 dB SPVL, $\sigma=4.4$ dB, n=74).

328 **3.3. Ratios between individual frequencies**

329 The most remarkable feature demonstrated by the individual tuning frequencies of the JO
330 units is the distinct relations between the ones belonging to the same recording site where a pair or a
331 triplet of units responded simultaneously. We divided the whole dataset in two parts, corresponding
332 to the pairs and triplets, and analyzed them independently.

333 The distribution of the ratio between the individual frequencies in the antiphase pairs
334 (n=85) is shown in Fig. 5A. The major peaks are centered around 1.2 and 1.25. The integer
335 representation of these values correspond to the ratios 6/5 and 5/4, respectively. The validity of
336 representation of frequency ratio in the form of a fractional ratio of integers is supported by the
337 values of the two minor peaks of the distribution: $1.17 \approx 7/6 = 1.16(6)$, $1.3 \approx 4/3 = 1.33(3)$.

338 The scatter of actual ratio values can be easily explained by the accuracy of measurements
339 in this study and the instability of frequency tuning in time: individual tuning frequencies were
340 measured to 1 Hz, while during the measurements the frequency could spontaneously change within
341 2 Hz range. Both factors affecting the F1/F2 ratio could shift the resulting value by 0.01, or two
342 bins of the histogram in Fig.5A, to either side of the mode. Within these limits, taken as the
343 predicted variation, the ratio of 5/4 was characteristic of 38 pairs of antiphase units.

344 In triplets of units (n=30) two of them demonstrated the in-phase autoexcitation, meaning
345 that each of the units received not only its own signal, converted to the vibration of the antenna, but
346 also the one of the second unit, recorded simultaneously. Such cumulative effect led to the
347 formation of a series of mixed harmonics in the recording. When the ratio between the frequencies
348 was close to 1.5 (3/2, one of the peaks in the distribution in Fig.5B), the resulting spectrum became
349 similar to a single harmonic series, like in Fig.2B. Such similarity complicated the identification of
350 the individual tuning frequencies in the in-phase pair of units; however, the primary frequency
351 could be distinguished from the mixed harmonics by the presence of the corresponding suppression

352 zone at the same frequency, appearing after the rotation of the stimulation vector by 180° , thus
353 converting the positive feedback to the negative one for a given unit (Lapshin and Vorontsov, 2017).

354 Figure 5B shows the distribution of frequency ratio F_3/F_2 from the triple systems ($n=30$). It
355 has several peaks, the most pronounced at 1.56, while the one corresponding to the integer ratio $3/2$
356 is lower. Similarly, in the distribution of the second frequency ratio from the same triplets (Fig. 5C)
357 dominates the peak centered at 1.22 which does not correspond to some obvious integer ratio, but
358 there are also peaks at $7/6$ and $6/5$ similar to the ones in Fig. 5A.

359 4. Discussion

360 4.1. Directional properties of the mosquito JO

361 The number of sensory units recorded in this study ($n=306$) represents only a minor part of
362 their overall number in the JO. However, even this random sample of units, most probably, could
363 perform the analysis of sound spectrum in all directions relative to the JO axis (Fig.4).

364 The average width of the directional characteristic is ca. 120° (Fig. 3B,D). Based on this
365 estimate, we can conclude that 4-5 similarly tuned units, evenly distributed around the axis in the
366 JO, would be enough to cover the whole directional range at the given frequency. However, this
367 could be insufficient to provide the required accuracy of determining the angular coordinates of the
368 sound source. According to Belton (1967) male mosquitoes are not attracted to the sounds which
369 come from larger distance, even if these signals contain conspecific female-like tones. For small
370 insects, the most accessible way to estimate the distance to a sound source is to measure its angular
371 position during their own displacement in space (parallax estimation of distance). In calm weather,
372 the swarming *C. p. pipiens* males fly longitudinal tracks. Analyzing the degree of parallax
373 displacement of a sound source, they, apparently, can determine the distance to this source. One can
374 presume that mosquitoes will pay attention to the sounds of nearby sources (within transverse size
375 of the swarm) while more or less ignoring the sounds coming from larger distance. This would help
376 to stabilize the position of the swarm and would increase the noise immunity of the male-female
377 auditory communication channel. However, the task of instant triangulation demands high speed
378 and precision of angular estimates performed by the JO, and can explain its seemingly redundant
379 complexity.

380 Unfortunately, we cannot be sure that the diagrams of the Fig.4 show the true angular distribution of
381 the differently tuned JO sensory units. The uncertainty lies in the possibility of selective recording
382 from certain parts of the antennal nerve due to the geometric constraints in mutual arrangement of
383 the mosquito, the recording electrode and the speaker. On the other hand, some asymmetry in the

384 angular distribution of sensory units still must be present, since mosquitoes with one antenna
385 maintained the ability, although much reduced, to locate a female (Roth, 1948).

386

387 **4.2. Pairs and triplets of sensory units**

388 Our measurements show that in the mosquito JO there is a large proportion of pairwise-
389 combined units with different frequency tuning and oppositely oriented polar patterns: 85% of
390 recorded units belonged to the paired or triple systems.

391 This finding means that during the single deflection of the antenna they generate antiphase
392 electrical signals. It is attractive to speculate that this physiological finding corresponds to the well-
393 known morphological fact that most sensillae in the JO contain two or three sensory cells (Boo and
394 Richards, 1975a; Hart et al., 2011) and that their axons keep adjacent position further to the
395 antennal nerve. The sinusoidal signals do not allow to separate responses of these two cells, but the
396 positive feedback stimulation provides an opportunity to study antiphase units separately and
397 measure their individual best frequencies and polar patterns.

398 How such antiphase responses are formed is currently unknown. We can propose at least
399 two hypothetic mechanisms: one is based on the initially different polarity of the mechano-electrical
400 transduction in the two cells belonging to a single sensilla, the other one – on the different and
401 precisely adjusted latency of signal transduction in the two cells. The latter mechanism is, however,
402 cannot work similarly in the wide range of frequencies. Currently we discard the third possibility –
403 that antiphase axons belong to the units from the opposite parts of the JO capsule – since there is no
404 morphological evidence of it.

405 The triple systems, including two units responding in-phase and the third one in antiphase,
406 give additional insight to the underlying neuronal morphology and support the above speculations.
407 Since in the triple-unit recordings the polar patterns of the in-phase pair were always oriented
408 similarly, with high degree of confidence it can be assumed that the units producing these responses
409 are morphologically combined in the capsule of the JO. Moreover, the specific ratio of best
410 frequencies in such pairs and triplets indicates the functional interaction between these units (Fig.5).

411 Morphological combination of two or more sensory cells into the sensilla is known for
412 many insect chordotonal organs (Field and Matheson, 1998), including the one of *Drosophila* flies,
413 Chironomidae midges and mosquitoes. From the widespread occurrence of this phenomenon among
414 insects, one can assume that it must have some general functional significance, not specific to the
415 mosquitoes. One of the possible tasks performed by such organization of the sensillae may be

416 preventing the auditory neurons from sending to the brain the responses to large low-frequency
417 deflections of the antenna caused by wind currents during the flight maneuvers of an insect. The
418 antiphase pair of sensory cells, having equal sensitivity in low-frequency range, can filter out such
419 signals even before they leave the JO or the antennal nerve, provided that these cells are
420 interconnected by gap junctions. The latter was indeed demonstrated in the JO of *Drosophila*
421 (Sivan-Loukianova and Eberl, 2005). Such mechanism must be very sensitive to the similarity of
422 parameters of both sensory cells. Combining them into a single sensilla is fully justified in order to
423 ensure equality of their directional characteristics and similarity of metabolism.

424 In a pairwise combination of specifically tuned antiphase units one can notice an analogy
425 with the opponent coding of color information in the vertebrate retina (Daw, 1973). The opponency
426 of auditory sensory units with different frequency tuning can substantially facilitate the following
427 information processing in the brain since it allows to easily distinguish the sounds with continuous
428 (noise-like) spectrum from the ones with line spectrum like the sound of a flying female, or to
429 produce selectivity for other stimulus features (Chang et al., 2016).

430

431 **4.3. Ratios between the individual frequencies**

432 The tendency of units in paired and triple systems to have their best frequency ratios equal
433 to the simple integer fractions (Fig.5) may be a sign of the mechanism of signal processing, some
434 kind of internal 'language' of the system, representing the auditory space of mosquito. Remarkably,
435 almost similar frequency ratios between the paired flight tones of male and female mosquitoes were
436 observed (Aldersley et al., 2016). Such tendency may also explain the multi-modal shape of overall
437 distribution of individual frequencies, which was demonstrated in our previous study (Lapshin and
438 Vorontsov, 2017).

439 It should be noted that in triple-unit systems the ratios between the individual frequencies
440 are interdependent. For example, if the ratio in the in-phase pair $F_3 / F_2 = 1.5$ and the ratio in any of
441 the antiphase pairs from the same triplet is, for example, $F_3 / F_1 = 1.25$, then the ratio in the other
442 antiphase pair should be equal to $F_1 / F_2 = 1.2$ ($F_1 / F_2 = F_3 / F_2 : F_3 / F_1$). However, there is a
443 possible alternative, when in triple systems the primary ones are the ratios in the antiphase pairs.
444 For example, if $F_1 / F_2 = 5/4$ and $F_3 / F_1 = 5/4$, then the third ratio between the in-phase units
445 becomes dependent: $F_3 / F_2 = 25/16 = 1.5625$. Similarly, with the two other frequency ratios
446 characteristic of the antiphase pairs equal to $F_1 / F_2 = 4/3 = 1.33(3)$ and $F_3 / F_1 = 7/6 = 1.166(6)$,
447 for the dependent in-phase pair we get $F_3 / F_2 = 14/9 = 1.55(5)$. Remarkably, in the Fig.5B the
448 above calculated ratios fall into the major peak of the distribution. Apparently, the frequency ratios

449 between the individual units in the triple systems do not follow clearly defined criteria (as it seems
450 they do in pairs of units, Fig. 5A), at the same time being distinctly non-random. Most probably,
451 they are limited by the more strict conditions which simultaneously connect three elements, for
452 example $F3 / F2 \times F3 / F1 = 1.22 \times 1.22 = 1.5$, or $1.22 \times 1.28 = 1.56$. Sub-peaks centered at these
453 values are indeed present in the distribution (Fig.5B,C).

454 The seeming complexity of frequency ratios in the JO may be explained in the framework
455 of primary signal processing. Since every sound, even the pure tone, comes to the JO sensory units
456 of a flying mosquito accompanied by mixed harmonics, there must be a demand to analyze this
457 complex auditory image and to simplify the input to the brain interneurons. Highly parallel system
458 of the JO sensory units supplemented by the ability to instantly discriminate the certain
459 combinations of tones seems to be almost perfectly suited for the task.

460 However, the complex pattern of frequency ratios that we observed could simply originate
461 from the known phenomenon of 'harmonic synchronization', that is the specific mode of interaction
462 between the coupled resonant nonlinear systems when their frequencies are integrally related to
463 each other. The stability of such synchronization is determined by the local decrease in the energy
464 of the entire system (Yang et al., 2012) and generally decreases with increasing frequency
465 multiplicity. One cannot exclude the hypothesis that the specific frequency ratios, including the
466 ones which manifest themselves in behavior, are not a part of signal processing mechanism of the
467 JO, but just a by-product of energy optimization.

468 However, regardless of the functional meaning of harmonic synchronization, it is possible
469 only if the oscillators express spontaneous activity at their best frequencies and interact,
470 mechanically or electrically. In the JO sensory cells the good candidate mechanism of interaction
471 would be the active auditory mechanics (Göpfert and Robert, 2001) based on the dynein – tubulin
472 motor of the ciliated sensillae (Warren et al., 2010). Such kind of interaction can also explain the
473 appearance of mixed harmonics visible in the sonograms of Fig2A.

474 Our recent finding suggests that mosquitoes can potentially demonstrate different kinds of
475 responses to different frequencies of sound. It was shown in behavioral tests that *Aedes diantaeus*
476 mosquitoes demonstrate fast avoidance response in the frequency range 140-200 Hz (Lapshin and
477 Vorontsov, 2018). In these experiments mosquitoes which were previously attracted by the sound
478 imitating the wingbeat tone of a female (280–320 Hz) left the stimulation area within one second
479 from the onset of the test signal (amplitude 57–69 dB SPVL), flying up, sideways and backward
480 relative to the direction of test signal arrival. These and other behavioral observations, together with

481 our current physiological findings, strongly suggest that the JO of mosquitoes can discriminate
482 tones coming from different directions in a wide range of amplitudes.

483

484 **5. Acknowledgments**

485 The field facilities for this study, Kropotovo biological station, was provided by the
486 Koltzov Institute of Developmental Biology RAS.

487 **6. Funding**

488 The work was conducted under the Government basic research programs, IITP RAS
489 № 0061-2016-0012 and IDB RAS 0108-2018-0002, and supported by RFBR grant 19-04-00628A.

490

491 **Figures**

492 **Fig 1. Experimental procedure.**

493 The experimental setup for electrophysiological recording and sound stimulation.

494 Mosquito is fixed above two orthogonally oriented speakers. Neuronal response from the
495 antennal nerve are amplified (1) and digitized (3) and stored on the PC (9). Sound stimulation is
496 made alternatively in feedback mode (neuronal response after phase adjustment (2) via attenuator
497 (4), power amplifier (5) and Sin-Cos transducer (6) is fed to speakers (7)) or sinusoidal mode
498 (signal is synthesized on the PC (9) and after digital-to-analog converter (8) is fed to attenuator (4)
499 and further to the speakers (7)). The mosquito is positioned at the intersection of axes of the two
500 speakers in such a way that the base of the antenna flagellum is perpendicular to the both axes. The
501 resulting direction of the air vibration velocity is determined by the vector superposition of the
502 signals from the two speakers. An increase in angle of stimulation φ corresponds to counter-
503 clockwise rotation of the velocity vector, with the insect's head viewed from the front. Accordingly,
504 when viewed from the mosquito's head along the antenna the clockwise rotation corresponds to the
505 increase in φ .

506

507 **Fig. 2. Examples of the JO unit responses to the feedback stimulation.**

508 A. The direction of sound wave is set to -60° , the feedback power is gradually increased
509 from the sub-threshold levels, above -4 dB the response appears first as the higher level of noise,

510 followed by sporadic bursts (from -1 to 0 dB) and continuous excitation at 172 Hz above 0 dB
511 (absolute threshold of autoexcitation 42 dB SPVL at the fundamental frequency). Then, the
512 stimulation is switched off, the direction of sound wave is rotated by 180° (to 120°) and the
513 procedure repeated starting from -10 dB. The auto-excitation this time appeared at 205 Hz,
514 threshold of autoexcitation 45 dB SPVL at the fundamental frequency. Continuous stripe at ca. 290
515 Hz represents the spontaneous activity in the JO, a correlate of active mechanics of the JO sensory
516 cells, and it produces the combination harmonic ($290-205=85$ Hz), which can be seen in the right
517 part of the sonogram.

518 B. An example of triple unit system responding to the rotation of sound vector. The
519 feedback level is kept constant 6 dB above the threshold of the first recorded unit (F1), the sound
520 vector is rotated by 360° in 15° steps. First autoexcitation frequency, F1, appeared at -135° and
521 disappeared at 15 (maximal level 52 dB at the fundamental frequency), then F2 (159 Hz, 50 dB)
522 and F3 (249 Hz, 51 dB) appeared at 45° and disappeared at -165° . Note the combination (mixed)
523 harmonics (F3-F2 and F2+F3) when two units were excited simultaneously. Arrows indicate the
524 moments when the autoexcitation appeared and disappeared.

525 Vertical axis: frequency, Hz, horizontal axis: time, minutes. Color represents the relative
526 amplitude of response.

527

528 **Fig. 3. Examples of polar patterns and directional characteristics measured from the**
529 **JO sensory units.**

530 A, polar patterns of a pair of antiphase units; best frequency of #1 is 201 Hz, of the #2 is
531 253 Hz.

532 B, the same pair of units as in A, diagram obtained with 230 Hz sinusoidal stimulation, the
533 threshold at the best direction is 29 dB SPVL.

534 C, polar pattern of the single unit, best frequency at 199 Hz.

535 D, the same unit as in C, directional diagram measured at 200 Hz, threshold 37 dB SPVL.

536 Angle of sound wave is shown at the perimeter of each diagram, measured from the dorso-
537 ventral axis (see Fig.1). Relative sensitivity is plotted radially in 3 dB (A) or 2 dB (B, C, D) steps.

538

539

540 **Fig. 4. Directional properties of the JO units.**

541 All data are given in polar coordinates with the center corresponding to the axis of the
542 antenna.

543 A, radial distribution of best frequencies of the JO units. Measurements are made from
544 polar patterns, obtained in the feedback stimulation mode, the individual tuning frequency values
545 are plotted radially. Filled circles show the higher-frequency units (F3) belonging to the triple-unit
546 systems. Histogram in the upper-left corner shows the total number of units recorded in each of the
547 quadrants.

548 B, radial distribution of individual thresholds. Measurements are made with sinusoidal
549 stimulation at previously determined individual best frequencies, inverse thresholds are plotted
550 radially, so the dots belonging to the higher sensitive units are further from the center of the graph.

551

552 **Fig. 5. Distributions of frequency ratio between the units.**

553 Individual frequencies are designated as F1 and F2 for pairs and F1, F2 and F3 for triplets,
554 where F1 unit is in antiphase to two in-phase units, lower (F2) and upper (F3) frequencies the
555 example response of such is given in Fig.2B). Numbers above the histograms show the rounded
556 values of the distribution local maxima and the respective integer ratios.

557 A, pairs of antiphase units, n=85. B, C, triplets of units, n=30. B, ratios in the in-phase
558 pairs. C, ratios in the antiphase pairs.

559

560 **References**

- Albert, J. T. and Göpfert, M. C.** (2015). Hearing in *Drosophila*. *Curr. Opin. Neurobiol.* **34**, 79–85.
- Aldersley, A. and Cator, L. J.** (2019). Female resistance and harmonic convergence influence male mating success in *Aedes aegypti*. *Sci. Rep.* **9**, 2145.
- Aldersley, A., Champneys, A., Homer, M. and Robert, D.** (2016). Quantitative analysis of harmonic convergence in mosquito auditory interactions. *J. R. Soc. Interface R. Soc.* **13**, 20151007.
- Belton, P.** (1967). Trapping mosquitoes with sound. *Proc. Pap. Thirty-Fifth Annu. Conf. Calif. Mosq. Control Assoc. Inc Am. Mosq. Control Assoc.* 98.
- Belton, P.** (1974). An analysis of direction finding in male mosquitoes. In *Experimental Analysis of Insect Behaviour* (ed. Browne, L. B.), pp. 139–148. Heidelberg, New York: Springer.

- Boo, K. S. and Richards, A. G.** (1975a). Fine structure of the scolopidia in the Johnston's organ of male *Aedes aegypti* (L.) (Diptera: Culicidae). *Int. J. Insect Morphol. Embryol.* **4**, 549–566.
- Boo, K. S. and Richards, A. G.** (1975b). Fine structure of scolopidia in Johnston's organ of female *Aedes aegypti* compared with that of the male. *J. Insect Physiol.* **21**, 1129–1139.
- Cator, L. J., Arthur, B. J., Harrington, L. C. and Hoy, R. R.** (2009). Harmonic convergence in the love songs of the dengue vector mosquito. *Science* **323**, 1077–1079.
- Chang, A. E. B., Vaughan, A. G. and Wilson, R. I.** (2016). A Mechanosensory Circuit that Mixes Opponent Channels to Produce Selectivity for Complex Stimulus Features. *Neuron* **92**, 888–901.
- Costello, R. A.** (1974). Effects of environmental and physiological factors on the acoustic behavior of *Aedes aegypti* (L.) (Diptera: Culicidae).
- Daley, D. L. and Camhi, J. M.** (1988). Connectivity pattern of the cercal-to-giant interneuron system of the American cockroach. *J. Neurophysiol.* **60**, 1350–1368.
- Daw, N. W.** (1973). Neurophysiology of color vision. *Physiol. Rev.* **53**, 571–611.
- Field, L. H. and Matheson, T.** (1998). Chordotonal Organs of Insects. In *Advances in Insect Physiology* (ed. Evans, P. D.), pp. 1–228. Academic Press.
- Gibson, G. and Russell, I.** (2006). Flying in tune: sexual recognition in mosquitoes. *Curr. Biol. CB* **16**, 1311–1316.
- Gibson, G., Warren, B. and Russell, I. J.** (2010). Humming in tune: sex and species recognition by mosquitoes on the wing. *J. Assoc. Res. Otolaryngol. JARO* **11**, 527–540.
- Göpfert, M. C. and Robert, D.** (2001). Active auditory mechanics in mosquitoes. *Proc. Biol. Sci.* **268**, 333–339.
- Hart, M., Belton, P. and Kuhn, R.** (2011). The Risler Manuscript. *Eur. Mosq. Bull.* **29**, 103–113.
- Hill, K. G. and Boyan, G. S.** (1976). Directional hearing in crickets. *Nature* **262**, 390–391.
- Kamikouchi, A., Inagaki, H. K., Effertz, T., Hendrich, O., Fiala, A., Göpfert, M. C. and Ito, K.** (2009). The neural basis of *Drosophila* gravity-sensing and hearing. *Nature* **458**, 165–171.
- Lapshin, D. N.** (2011). Frequency threshold curves of auditory interneurons of male mosquitoes *Culex pipiens pipiens* L. (Diptera, Culicidae). *Dokl. Biol. Sci.* **439**, 191–193.
- Lapshin, D. N.** (2012). Mosquito Bioacoustics: Auditory Processing in *Culex pipiens pipiens* L. males (Diptera, Culicidae) during Flight Simulation. *Entomol. Rev.* **92**, 605–621.
- Lapshin, D. N.** (2015). Directional and frequency characteristics of auditory receptors in midges (Diptera, Chironomidae). *Entomol. Rev.* **95**, 1155–1165.
- Lapshin, D. N. and Vorontsov, D. D.** (2013). Frequency tuning of individual auditory receptors in female mosquitoes (Diptera, Culicidae). *J. Insect Physiol.* **59**, 828–839.
- Lapshin, D. N. and Vorontsov, D. D.** (2017). Frequency organization of the Johnston's organ in male mosquitoes (Diptera, Culicidae). *J. Exp. Biol.* **220**, 3927–3938.

- Lapshin, D. N. and Vorontsov, D. D.** (2018). Low-Frequency Sounds Repel Male Mosquitoes *Aedes diaantaeus* N.D.K. (Diptera, Culicidae). *Entomol. Rev.* **98**, 266–271.
- Matsuo, E. and Kamikouchi, A.** (2013). Neuronal encoding of sound, gravity, and wind in the fruit fly. *J. Comp. Physiol. A Neuroethol. Sens. Neural. Behav. Physiol.* **199**, 253–262.
- Morley, E. L., Steinmann, T., Casas, J. and Robert, D.** (2012). Directional cues in *Drosophila melanogaster* audition: structure of acoustic flow and inter-antennal velocity differences. *J. Exp. Biol.* **215**, 2405–2413.

- Pennetier, C., Warren, B., Dabiré, K. R., Russell, I. J. and Gibson, G.** (2010). “Singing on the wing” as a mechanism for species recognition in the malarial mosquito *Anopheles gambiae*. *Curr. Biol. CB* **20**, 131–136.
- Robert, D.** (2005). Directional Hearing in Insects. In *Sound Source Localization* (ed. Popper, A. N.) and Fay, R. R.), pp. 6–35. New York, NY: Springer New York.
- Roth, L. M.** (1948). A Study of Mosquito Behavior. An Experimental Laboratory Study of the Sexual Behavior of *Aedes aegypti* (Linnaeus). *Am. Midl. Nat.* **40**, 265–352.
- Simões, P. M. V., Ingham, R. A., Gibson, G. and Russell, I. J.** (2016). A role for acoustic distortion in novel rapid frequency modulation behaviour in free-flying male mosquitoes. *J. Exp. Biol.* **219**, 2039–2047.
- Simões, P. M. V., Ingham, R., Gibson, G. and Russell, I. J.** (2018). Masking of an auditory behaviour reveals how male mosquitoes use distortion to detect females. *Proc. Biol. Sci.* **285**, 20171862.
- Sivan-Loukianova, E. and Eberl, D. F.** (2005). Synaptic Ultrastructure of *Drosophila* Johnston’s Organ Axon Terminals as Revealed by an Enhancer Trap. *J. Comp. Neurol.* **491**, 46–55.
- Sotavalta, O.** (1952). Flight-Tone and Wing-Stroke Frequency of Insects and the Dynamics of Insect Flight. *Nature* **170**, 1057.
- Theunissen, F., Roddey, J. C., Stufflebeam, S., Clague, H. and Miller, J. P.** (1996). Information theoretic analysis of dynamical encoding by four identified primary sensory interneurons in the cricket cercal system. *J. Neurophysiol.* **75**, 1345–1364.
- Vedenina, V. Y., Rozhkova, G. I., Panjutin, A. K., Byzov, A. L. and Kämper, G.** (1998). Frequency-intensity characteristics of cricket cercal interneurons: low-frequency-sensitive units. *J. Comp. Physiol. A* **183**, 553–561.
- Villarreal, S. M., Winokur, O. and Harrington, L.** (2017). The Impact of Temperature and Body Size on Fundamental Flight Tone Variation in the Mosquito Vector *Aedes aegypti* (Diptera: Culicidae): Implications for Acoustic Lures. *J. Med. Entomol.* **54**, 1116–1121.
- Warren, B., Gibson, G. and Russell, I. J.** (2009). Sex Recognition through midflight mating duets in *Culex* mosquitoes is mediated by acoustic distortion. *Curr. Biol. CB* **19**, 485–491.
- Warren, B., Lukashkin, A. N. and Russell, I. J.** (2010). The dynein-tubulin motor powers active oscillations and amplification in the hearing organ of the mosquito. *Proc. Biol. Sci.* **277**, 1761–1769.
- Yang, N., Long, Z. and Wang, F.** (2012). Harmonic synchronization model of the mating dengue vector mosquitoes. *Chin. Sci. Bull.* **57**, 4043–4048.
- Yorozu, S., Wong, A., Fischer, B. J., Dankert, H., Kernan, M. J., Kamikouchi, A., Ito, K. and Anderson, D. J.** (2009). Distinct sensory representations of wind and near-field sound in the *Drosophila* brain. *Nature* **458**, 201–205.

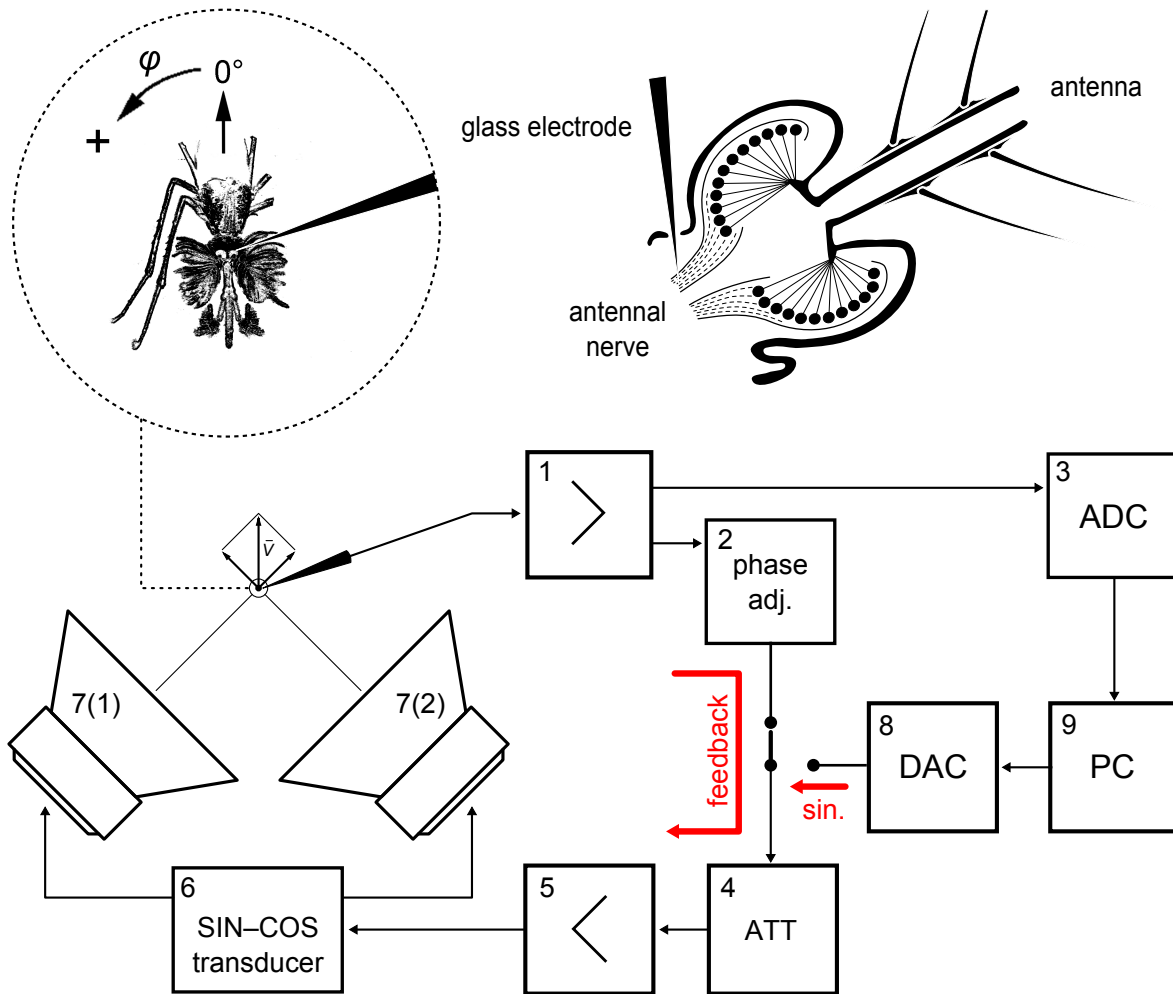


Fig 1. Experimental procedure.

The experimental setup for electrophysiological recording and sound stimulation.

Mosquito is fixed above two orthogonally oriented speakers. Neuronal response from the antennal nerve are amplified (1) and digitized (3) and stored on the PC (9). Sound stimulation is made alternatively in feedback mode (neuronal response after phase adjustment (2) via attenuator (4), power amplifier (5) and Sin-Cos transducer (6) is fed to speakers (7)) or sinusoidal mode (signal is synthesized on the PC (9) and after digital-to-analog converter (8) is fed to attenuator (4) and further to the speakers (7)). The mosquito is positioned at the intersection of axes of the two speakers in such a way that the base of the antenna flagellum is perpendicular to the both axes. The resulting direction of the air vibration velocity is determined by the vector superposition of the signals from the two speakers. An increase in angle of stimulation ϕ corresponds to counter-clockwise rotation of the velocity vector, with the insect's head viewed from the front. Accordingly, when viewed from the mosquito's head along the antenna the clockwise rotation corresponds to the increase in ϕ .

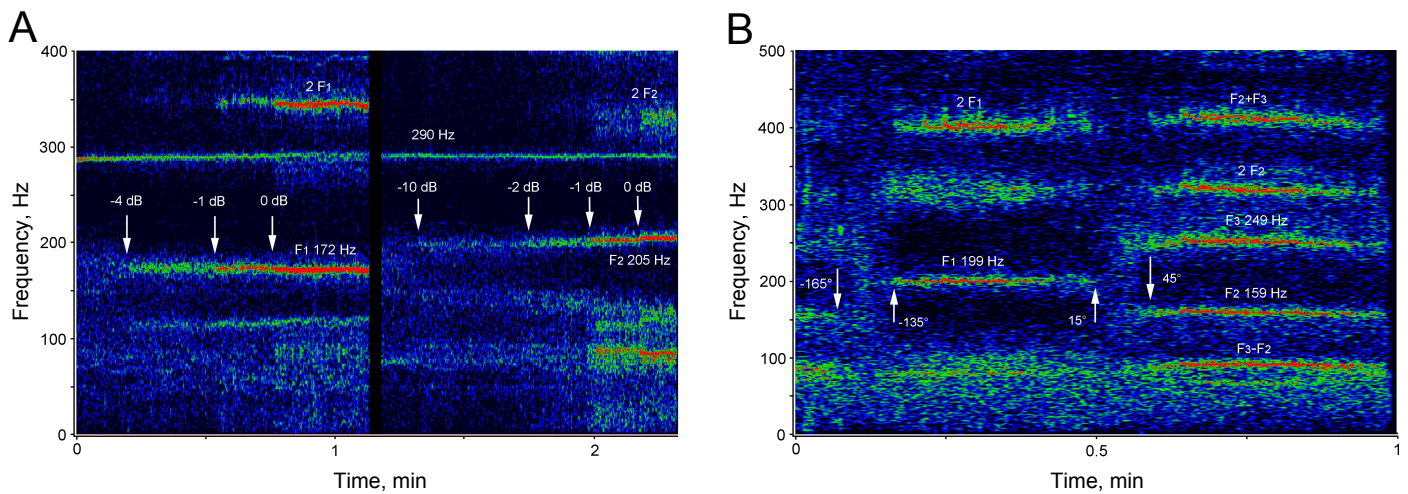


Fig. 2. Examples of the JO unit responses to the feedback stimulation.

A. The direction of sound wave is set to -60° , the feedback power is gradually increased from the sub-threshold levels, above -4 dB the response appears first as the higher level of noise, followed by sporadic bursts (from -1 to 0 dB) and continuous excitation at 172 Hz above 0 dB (absolute threshold of autoexcitation 42 dB SPVL at the fundamental frequency). Then, the stimulation is switched off, the direction of sound wave is rotated by 180° (to 120°) and the procedure repeated starting from -10 dB. The auto-excitation this time appeared at 205 Hz, threshold of autoexcitation 45 dB SPVL at the fundamental frequency. Continuous stripe at ca. 290 Hz represents the spontaneous activity in the JO, a correlate of active mechanics of the JO sensory cells, and it produces the combination harmonic ($290-205=85$ Hz), which can be seen in the right part of the sonogram.

B. An example of triple unit system responding to the rotation of sound vector. The feedback level is kept constant 6 dB above the threshold of the first recorded unit (F1), the sound vector is rotated by 360° in 15° steps. First autoexcitation frequency, F1, appeared at -135° and disappeared at 15° (maximal level 52 dB at the fundamental frequency), then F2 (159 Hz, 50 dB) and F3 (249 Hz, 51 dB) appeared at 45° and disappeared at -165° . Note the combination (mixed) harmonics (F3-F2 and F2+F3) when two units were excited simultaneously. Arrows indicate the moments when the autoexcitation appeared and disappeared. Vertical axis: frequency, Hz, horizontal axis: time, minutes. Color represents the relative amplitude of response.

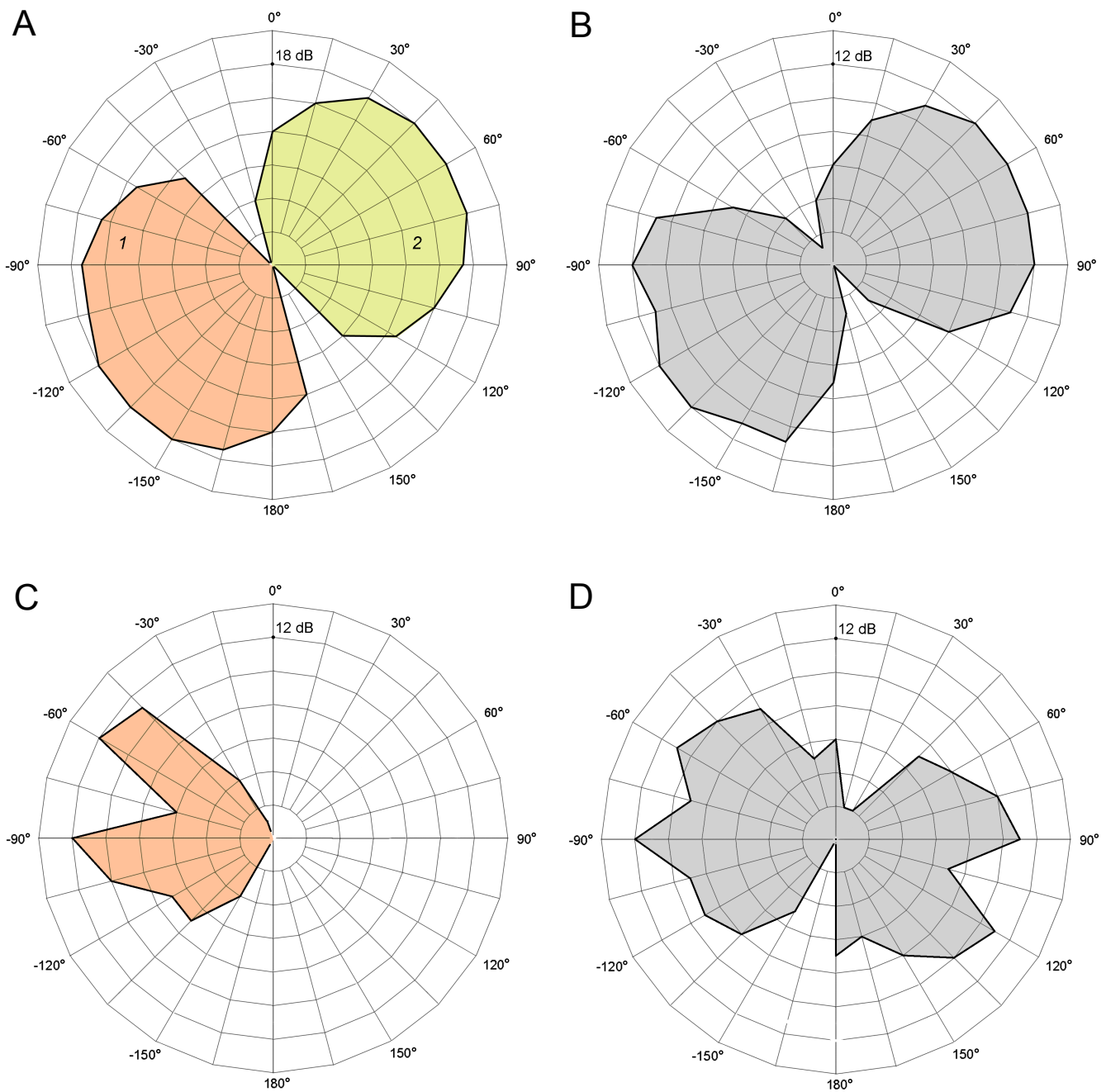


Fig. 3. Examples of polar patterns and directional characteristics measured from the JO sensory units.

A, polar patterns of a pair of antiphase units; best frequency of #1 is 201 Hz, of the #2 is 253 Hz.

B, the same pair of units as in A, diagram obtained with 230 Hz sinusoidal stimulation, the threshold at the best direction is 29 dB SPVL.

C, polar pattern of the single unit, best frequency at 199 Hz.

D, the same unit as in C, directional diagram measured at 200 Hz, threshold 37 dB SPVL.

Angle of sound wave is shown at the perimeter of each diagram, measured from the dorso-ventral axis (see Fig.1). Relative sensitivity is plotted radially in 3 dB (A) or 2 dB (B, C, D) steps.

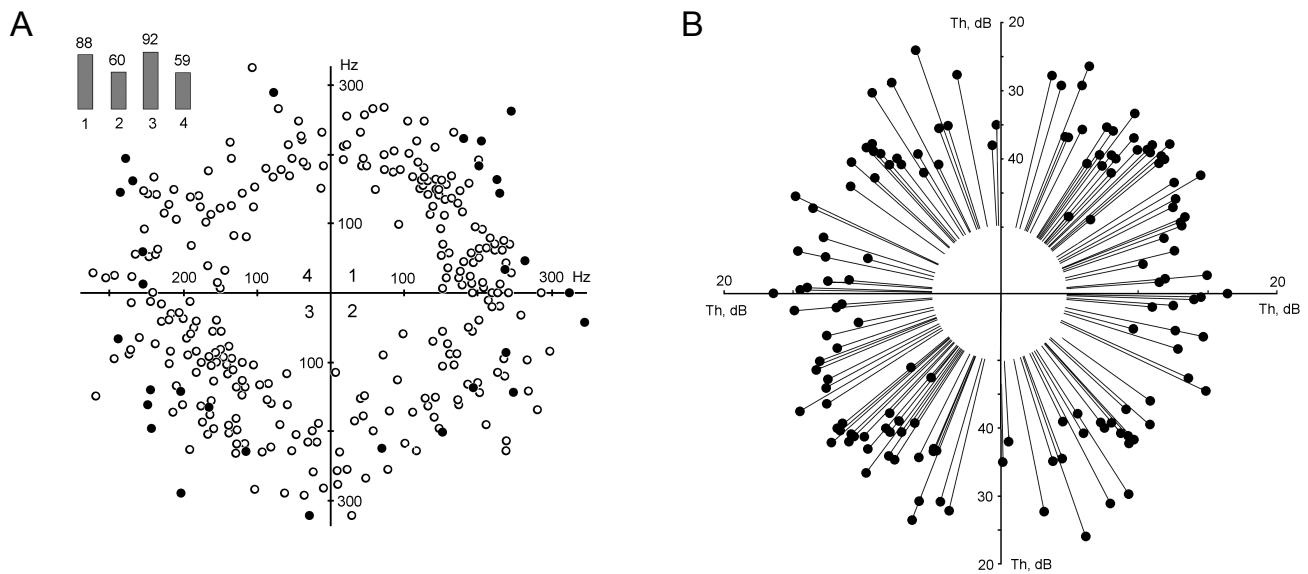


Fig. 4. Directional properties of the JO units.

All data are given in polar coordinates with the center corresponding to the axis of the antenna.

A, radial distribution of best frequencies of the JO units. Measurements are made from polar patterns, obtained in the feedback stimulation mode, the individual tuning frequency values are plotted radially. Filled circles show the higher-frequency units (F3) belonging to the triple-unit systems. Histogram in the upper-left corner shows the total number of units recorded in each of the quadrants.

B, radial distribution of individual thresholds. Measurements are made with sinusoidal stimulation at previously determined individual best frequencies, inverse thresholds are plotted radially, so the dots belonging to the higher sensitive units are further from the center of the graph.

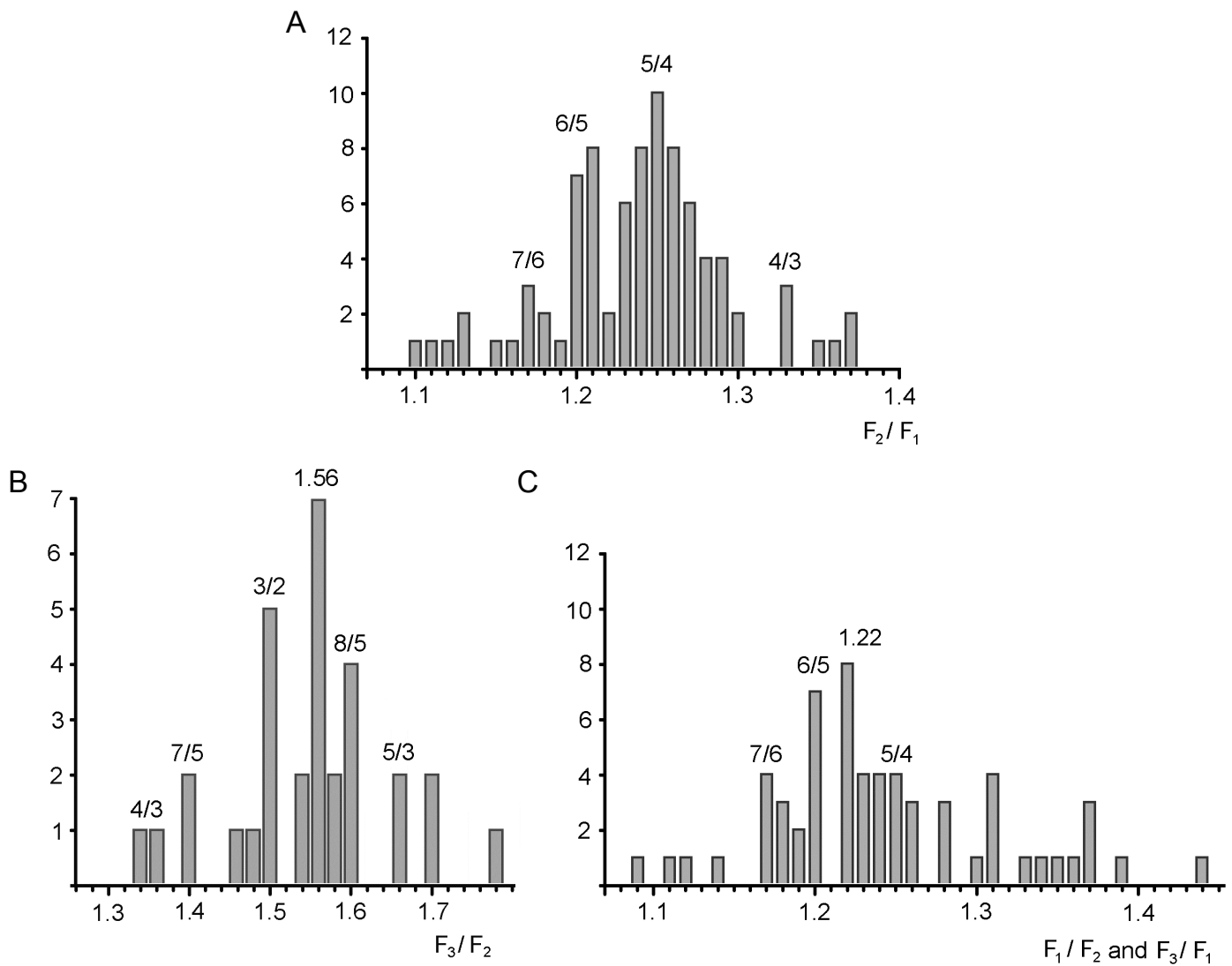


Fig. 5. Distributions of frequency ratio between the units.

Individual frequencies are designated as F1 and F2 for pairs and F1, F2 and F3 for triplets, where F1 unit is in antiphase to two in-phase units, lower (F2) and upper (F3) frequencies the example response of such is given in Fig.2B). Numbers above the histograms show the rounded values of the distribution local maxima and the respective integer ratios.

A, pairs of antiphase units, n=85. B, C, triplets of units, n=30. B, ratios in the in-phase pairs. C, ratios in the antiphase pairs.